2002

Overexpression and Divalent Metal Binding Properties of the Methionyl Aminopeptidase from *Pyrococcus furiosus*

Lu Meng
Utah State University

Shane Ruebush
Utah State University

Ventris M. D'Souza
Utah State University

Alicja J. Copik
Utah State University

Susumu Tsunasawa
BioCollege Kyoto

See next page for additional authors

Overexpression and Divalent Metal Binding Properties of the Methionyl Aminopeptidase from *Pyrococcus furiosus*

Lu Meng
Department of Chemistry and Biochemistry, Utah State University, Logan, Utah
Shane Ruebush
Department of Chemistry and Biochemistry, Utah State University, Logan, Utah
Ventris M. D'souza
Department of Chemistry and Biochemistry, Utah State University, Logan, Utah
Alicja J. Copik
Department of Chemistry and Biochemistry, Utah State University, Logan, Utah
Susumu Tsunasawa
BioCollege Kyoto, Kamigyoh District, Kyoto, Japan
Richard C. Holz
Department of Chemistry and Biochemistry, Utah State University, Logan, Utah

SUBJECTS:

Peptides and proteins, Metals, Monomers, Ions, Screening assays

Abstract

The gene encoding for the methionyl aminopeptidase from the hyperthermophilic archaeon *Pyrococcus furiosus* (*Pf*MetAP-II; EC 3.4.11.18) has been inserted into a pET 27b(+) vector and overexpressed in *Escherichia coli*. The new expression system resulted in a 5-fold increase in purified enzyme obtained from a 5 L fermentor growth. The as-purified *Pf*MetAP-II enzyme, to which no exogenous metal ions or EDTA was added, was found to have 1.2 equiv of zinc and 0.1 equiv of iron present by ICP-AES analysis. This enzyme had a specific activity of 5 units/mg, a 60-fold decrease from the fully loaded Fe(II) enzymes. When an additional 2 equiv of Zn(II) was added to the as-purified *Pf*MetAP-II, no activity could be detected. The combination of these data with previously reported whole cell studies on *Ec*MetAP-I further supports the suggestion that the in vivo metal ion for all MetAP's is Fe(II). Both Co(II)- and Fe(II)-loaded *Pf*MetAP-II showed similar substrate specificities to *Ec*MetAP-I. Substrate binding was largely affected by the amino acid in the P1 position and the length of the polypeptide. The substrates MSSHRWDW and MP-*p*-NA showed the smallest K_m values while the substrates MGMM and MP-*p*-NA provided the highest turnover. The catalytic efficiency (k_{cat}/K_m) of *Pf*MetAP-II for MP-*p*-NA at 30 °C was 799 500 and 340 930 M^{-1} s^{-1} for Co(II)- and Fe(II)-loaded *Pf*MetAP-II, respectively. Maximum catalytic activity was obtained with 1 equiv of Co(II) or Fe(II), and the dissociation constants (K_d) for the first metal binding site were found to be 50 ± 15 and 20 ± 15 nM for Co(II)- and Fe(II)-substituted *Pf*MetAP-II, respectively. Electronic absorption spectral titration of a 1 mM sample of apo-*Pf*MetAP-II with Co(II) provided a dissociation constant of 0.35 ± 0.02 mM for the second metal binding site, a 17500-fold increase compared to the first metal binding site. The electronic absorption data also indicated that both Co(II) ions reside in a pentacoordinate geometry. *Pf*MetAP-II shows unique thermostability and the optimal temperature for substrate turnover was found to be ∼85 °C at pH 7.5 in 25 mM Hepes and 150 mM KCl buffer. The hydrolysis of MGMM was measured in triplicate between 25 and 85 °C at eight substrate concentrations ranging from 2 to 20 mM. Both specific activity and K_m values increased with increasing temperature. An Arrhenius plot was constructed from the k_{cat} values and was found to be linear over the temperature range 25−85 °C, indicating that the rate-limiting step in *Pf*MetAP-II peptide hydrolysis does not change as a function of temperature. Co(II)- and Fe(II)-loaded *Pf*MetAP-II have similar activation energies (13.3 and 19.4 kJ/mol, respectively). The thermodynamic parameters calculated at 25 °C are as follows: $\Delta G^{\ddagger}$ = 46.23 kJ/mol, $\Delta H^{\ddagger}$ = 10.79 kJ/mol, and $\Delta S^{\ddagger}$ = −119.72 $J \cdot mol^{-1} \cdot K^{-1}$ for Co(II)-loaded *Pf*MetAP; $\Delta G^{\ddagger}$ = 46.44 kJ/mol, $\Delta H^{\ddagger}$ = 16.94 kJ/mol, and $\Delta S^{\ddagger}$ = −99.67 $J \cdot mol^{-1} \cdot K^{-1}$ for Fe(II)-loaded *Pf*MetAP. Interestingly, at higher temperatures (>50 °C), Fe(II)-loaded *Pf*MetAP-II is more active (1.4-fold at 85 °C) than Co(II)-loaded *Pf*MetAP-II.

Methionyl aminopeptidases (MetAP's)[1] represent a unique class of proteases that are capable of the hydrolytic removal of N-terminal methionine residues from nascent polypeptide chains (*1*−*4*). In prokaryotes, mitochondria, and chloroplasts the initiator residue is an *N*-formyl methionine group. The *N*-formyl group is removed from proteins in prokaryotes and eukaryotic organelles by a deformylase, leaving a methionine residue at the amino terminus (*2*). Many mature proteins do not retain an N-terminal methionine residue since they require modifications and/or processing during and after translation (*5*). Examples include the removal of signal sequences, proteolytic cleavage to generate shorter peptides, and the covalent attachment of residues and blocking groups (e.g., acetyl and myristoyl groups). The structure of the mature N-terminus plays a critical role in

N-directed degradation pathways and in targeting cellular membranes (*1*−*4*). The physiological importance of MetAP activity is underscored by the fact that deletion of MetAP genes in *Escherichia coli*, *Salmonella typhimurium*, and *Saccharomyces cerevisiae* is lethal to the cell (*6*−*8*). Moreover, MetAP's have recently been identified as the molecular target for the epoxide-containing antiangiogenesis agents TNP-470 and fumagillin, one of which is in phase III clinical trials (*9*−*13*). Therefore, MetAP's represent an important target for the development of novel anticancer, antibacterial, and/or antifungal agents.

MetAP's are organized into two classes (type I and type II) on the basis of the absence or presence of a 62 amino acid sequence inserted near the C-terminus. The function of this insert has yet to be established. The MetAP's from *E. coli* (type I), *Homo sapiens* (type II), and *Pyrococcus furiosus* (type II) have been crystallographically characterized (*13*−*16*). All three have been shown to have identical catalytic domains that contain a bis(μ-carboxylato)(μ-aquo/hydroxo)dicobalt core with an additional carboxylate residue at each metal site and a single histidine residue bound to one of the two metal ions (*13*−*16*). Since all of the catalytic domain residues are completely conserved in both type I and type II MetAP's, all MetAP's should bind divalent metal ions similarly. With this in mind, it was recently suggested that the in vivo metal ion for the type I MetAP from *E. coli* (*Ec*MetAP-I) is Fe(II) on the basis of whole cell metal analyses, activity measurements, and substrate binding constants (*17, 18*). In addition, the observed catalytic activity as a function of divalent metal ion and the metal binding constants for both Fe(II) and Co(II) *Ec*MetAP-I led to the proposal that MetAP's function as mononuclear enzymes in vivo, which was recently corroborated by extended X-ray absorption fine structure (EXAFS) spectroscopy (*17, 19*). The high-affinity or catalytically relevant metal binding site was assigned as the histidine-containing site. However, Yang et al. (*20*) more recently suggested that the type II MetAP from *H. sapiens* (*Hs*MetAP-II) binds divalent metal ions differently from type I MetAP enzymes in that *Hs*MetAP-II requires two Co(II) ions to be fully activated (*20*).

To understand the reported differences in the divalent metal binding properties between type I and type II MetAP's, we have examined how the type II MetAP from *P. furiosus* (*Pf*MetAP-II) binds divalent metal ions. *Pf*MetAP-II is by far the most thermostable member of the MetAP family of enzymes, with an optimum catalytic activity around 85 °C with a half-life of approximately 4.5 h (*21*). *Pf*MetAP-II and *Hs*MetAP-II are 39% identical while *Pf*MetAP-II and *Ec*MetAP-I are 33% identical, suggesting that structural and mechanistic data obtained for *Pf*MetAP-II will likely be similar to that determined for *Hs*MetAP-II and *Ec*MetAP-I. To further examine the structure and function of *Pf*MetAP-II, a new expression system for the *Pf*MetAP-II gene was developed that produces five times more enzyme than the previously reported overexpression system. We have also examined the substrate specificity, metal binding properties, and temperature dependence of the catalytic activity of *Pf*MetAP-II in the presence of either Co(II) or Fe(II). Comparison of the data presented herein with other MetAP's suggests that both type I and type II MetAP's bind divalent metal ions in an identical fashion and are likely mononuclear Fe(II)-dependent metalloproteases.

Materials and Methods

Purification of Recombinant PfMetAP-II.

*Pf*MetAP-II was purified similarly to that previously reported with minor modifications (*21*). Briefly, frozen cells (∼35 g) were thawed and suspended in 100 mL of 20 mM Tris-HCl buffer, pH 7.5. To this solution were added 0.5 mL of 100 mM PMSF, 4.5 mg of lysozyme, 4.5 mg of DNase I, and 10 μL of 1 M $MgCl_2$. This solution was stirred for 30 min at 25 °C followed by cooling to 4 °C for 1 h. This cell solution was sonicated in 50 mL aliquots for three 1 min intervals with ∼2 min intervals on ice. The mixture was then heated for 10 min at 100 °C. After centrifugation at 18000 rpm for 45 min, the supernatant was concentrated by ultrafiltration using an Amicon YM 10 membrane and dialyzed against 20 mM phosphate buffer, pH 8.0, overnight, with two buffer changes. The dialyzate was loaded onto a DEAE-Sepharose CL-6B column (Pharmacia, 2.5 × 16 cm) equilibrated with 20 mM

phosphate buffer, pH 8.0. The protein was eluted at a flow rate of 1 mL/min with a linear gradient of 0−0.5 M KCl. The fractions containing *Pf*MetAP-II were identified by SDS−PAGE, combined and concentrated to ∼20 mL, and then dialyzed against 10 mM phosphate buffer at pH 7.0 overnight. This dialyzate was loaded onto a CM-Sepharose CL-6B column (Pharmacia, 1.5 × 12 cm) equilibrated with phosphate buffer at pH 7.0. A linear gradient of 0−0.5 M KCl was used to elute the protein. Fractions containing *Pf*MetAP-II were concentrated to 3−4 mL using a Centriprep-10 (Millipore Corp.) and then loaded onto a gel filtration column (Sephadex 75 Hi-load prep-grade 16/60, Pharmacia) equilibrated with phosphate buffer at pH 7.0, containing 0.2 M KCl, at a flow rate of 0.3 mL/min. Purified *Pf*MetAP-II exhibited a single band on a SDS−PAGE, providing a M_r of 32850. Protein concentrations were estimated from the absorbance at 280 nm using an extinction coefficient of 21650 M^{-1} cm^{-1}.

Metal-free *Pf*MetAP-II was prepared by concentrating the as-purified *Pf*MetAP-II to a volume of ∼5 mL, after which EDTA was added to a final concentration of 10 mM. The resulting protein solution was dialyzed against 25 mM Hepes buffer (2 L, pH 7.5) containing 10 mM EDTA and 150 mM KCl at 4 °C for 2 days with two buffer changes per day. The protein solution was then dialyzed against chelexed (Chelex-100 Column) 25 mM Hepes buffer (2 L, pH 7.5) containing 150 mM KCl for 3 days against two buffer changes per day. The resulting *Pf*MetAP-II was inactive and was found to contain no detectable metal ions via inductively coupled plasma atomic emission spectrometry (ICP-AES). This enzyme deemed “apo-*Pf*MetAP-II” was stored at −80 °C.

Metal Content Measurements.

Enzyme samples for metal analysis were typically 30 μM. Apo-*Pf*MetAP-II samples were incubated under anaerobic conditions with Co(II) or Fe(II) ($CoCl_2$ or $FeSO_4$, ≥99.999%; Strem Chemicals, Newburyport, MA) for 30 min prior to exhaustive dialysis under anaerobic conditions against Chelex-treated buffer as previously reported (*17, 18*). Metal analyses were performed using ICP-AES.

Enzymatic Assay of PfMetAP-II.

All assays were performed under strict anaerobic conditions in an inert atmosphere glovebox (Coy) with a dry bath incubator to maintain the temperature. Catalytic activities were determined with an error of ±5%. Enzyme activity was determined in 25 mM Hepes buffer, pH 7.5, containing 150 mM KCl with different substrates (MGMM, MAS, and MSSHRWDW). The amount of product formation was determined by high-performance liquid chromatography (HPLC; Shimadzu LC-10A Class-VP5). Metal-substituted *Pf*MetAP-II samples were prepared by adding 3 equiv of the appropriate divalent metal ion to a buffered solution of 10 μM apo-*Pf*MetAP-II, and the mixture was incubated at 30 °C for 30 min. A typical assay involved the addition of 4 μL of M(II)-loaded *Pf*MetAP-II to a 16 μL substrate−buffer mixture followed by incubation at 30 °C for 1 min. The reaction was quenched by the addition of 20 μL of 1% trifluoroacetic acid solution (TFA). The elution of the products was monitored at 215 nm following separation on a C8 HPLC column (Phenomenex, Luna; 5 μm, 4.6 × 25 cm). Gradient elution was used at 1.5 mL/min. For the substrates MAS and MGMM, solvent A was 0.1% TFA in water, and solvent B was 50% Nanopure water, 50% HPLC-grade acetonitrile, and 0.1% TFA. For MGMM the starting gradient was 95/5 (A/B), and after 2 min the concentration of solvent B was increased from 5% to 100% over 10 min. The eluent mixture was held at 100% solvent B for an additional 2 min. Then the gradient was decreased to 5% in one second and continued to run at 5% solvent B for 2 min. The product GMM eluted around 10.7 min, and the substrate MGMM was eluted at around 11.8 min. For substrate MAS, the starting gradient was 100/0 (A/B). The gradient was increased from 0% to 5% solvent B within 2 min and then from 5% to 8% in 1 min; solvent B was increased from 8% to 50% in 5 min and then increased to 100% in the next 2 min. After running 100% solvent B for 2 min, 100% solvent A was run for another 2 min. The product AS was eluted at 2.6 min, and the substrate MAS was eluted at about 8.6 min. For the octapeptide MSSHRWDW, 98% water, 2% acetonitrile, and 0.1% TFA were used as mobile phase A and 100% acetonitrile and 0.1% TFA as mobile phase B. The gradient was increased from 0% to 17% solvent B during the first 2 min and then increased to 27% over the next 16 min, followed by 100% solvent B for 2 min; 100% solvent A was added for another 5 min. The product SSHRWDW was

eluted at about 15.5 min, and the substrate MSSHRWDW was eluted at about 16.5 min. Activity was determined on the basis of the amount of product (AS, GMM, or SSHRWDW) formed using a standard curve generated by running HPLC chromatograms of known concentrations of the dipeptide, tripeptide, and heptapeptide.

The kinetic parameters *V* (velocity) and K_m (Michaelis constant) were determined in triplicate. Enzyme activities are expressed as units per milligram, where one unit is defined as the amount of enzyme that releases 1 μmol of product at 30 °C in 1 min. The metal binding titration and temperature dependence reactions were carried out using the same conditions as determined for the kinetic constants. The hydrolysis of MP-*p*-NA was monitored spectrophotometrically at 405 nm on the basis of the increase in absorbance of *p*-NA ($\Delta\varepsilon_{405}$ value of *p*-nitroaniline of 10600 M^{-1} cm^{-1}) (*18*). The reaction mixture consisted of 5 μL of 10 μM enzyme solution, 3 μL of 2.0 mM prolidase, and substrate solution in different concentrations to a final volume of 1000 μL. One unit was defined as the amount of enzyme that releases 1 μmol of *p*-NA at 25 °C in 1 min.

Spectroscopic Measurements.

Electronic absorption spectra were recorded on a Shimadzu UV-3101PC spectrophotometer. All apo-*Pf*MetAP-II samples used in spectroscopic measurements were rigorously degassed prior to incubation with Co(II) or Fe(II) ($CoCl_2$ or $FeSO_4$, ≥99.999%; Strem Chemicals, Newburyport, MA) for ∼30 min at 25 °C. All Co(II)- and Fe(II)-containing samples were handled in an anaerobic glovebox (95% N_2/5% H_2, ≤1 ppm of O_2; Coy Laboratories). Electronic absorption spectra were normalized for the protein concentration and the absorption due to uncomplexed Co(II) ($\varepsilon_{512\ nm}$ = 6.0 M^{-1} cm^{-1}).

Results

Overexpression and Purification of PfMetAP-II.

The original culture of *E. coli* strain JM109 carrying the plasmid containing the gene for *Pf*MetAP-II showed low levels of expression that were insufficient for detailed kinetic and spectroscopic studies (*21*). To increase the yield of *Pf*MetAP-II, the *Pf*MetAP-II gene was cloned and placed into a pET 27b(+) expression vector. The original vector containing the *Pf*MetAP-II gene was isolated using a Wizard Plus Miniprep DNA purification kit (Promega). The plasmid was used as the template for PCR (PCR Kit, Amersham Pharmacia Biotech Inc.) to engineer restriction sites for *Nde*I and *Sal*I using primers synthesized by Operon Technologies. The primers used were the follows: upper primer, 5‘-GTC TGG CAT ATG GAT ACT GAA AAA CTT-3‘ (*Nde*I restriction site underlined); lower primer, 5‘-GCT GAG GTC GAC TCA TTC TGT CGT CAC TAT-3‘ (*Sal*I restriction site underlined). The PCR product of 0.9 kbp was purified on and excised from an agarose gel using a Qiaex Gel Extraction Kit (Qiagen) (Figure 1). The gene was sequenced and was identical to that previously reported for *Pf*MetAP-II. The PCR product was inserted into a pGEM-T easy cloning vector (Promega). Isolated plasmid was digested with the restriction enzymes *Nde*I and *Sal*I and ligated into the pET 27b(+) expression vector that had been digested with *Nde*I and *Sal*I (Novagen). This plasmid was transformed into BL21 *E. coli* cells. Transformants were again screened using restriction digests, and IPTG induced protein overexpression of *E. coli* BL21 cells grown in a shake flask for 12−14 h at 37 °C, containing 15 mg of kanamycin. Cells were grown in a 5 L fermentor at 37 °C with an air flow of 12 L/min to which 1 mM IPTG was added to induce protein expression at an OD_{600} of 1.0. The cells were allowed to grow for 3 h to 28 °C and then harvested by centrifugation at 8000 rpm for 15 min at 4 °C. After overexpression and purification, the increase in protein production from a 5 L fermentor was 5-fold, allowing 100 mg of purified *Pf*MetAP-II to be obtained from 5 L.

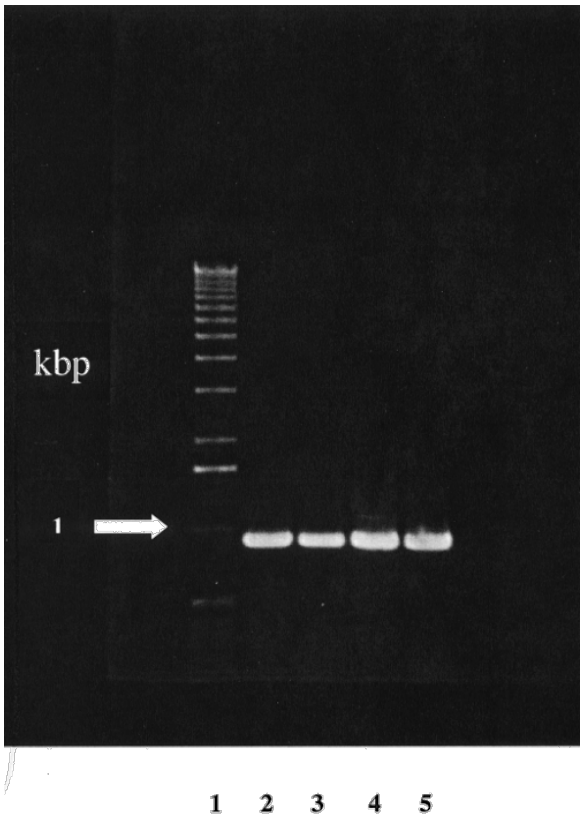

Figure 1 Agarose gel of the *Pf*MetAP-II gene after PCR. Lane 1 is the molecular weight marker, and lanes 2−5 are the 0.9 kbp gene encoding for *Pf*MetAP-II.

Analyses of the Metal Ion Content of PfMetAP-II.

The metal content of purified *Pf*MetAP-II, to which no supplemental metal ions or EDTA had been added throughout the cellular growth and purification process, contained 1.2 equiv of zinc and 0.1 equiv of iron. No cobalt was detected. The specific activity of this enzyme at 30 °C, pH 7.5, using MGMM as the substrate was 5.0 units/mg, which is ∼60 times less active than either the Co(II)- or Fe(II)-loaded *Pf*MetAP-II enzyme.

The number of tightly bound divalent metal ions was determined for *Pf*MetAP-II by ICP-AES analysis. *Pf*MetAP-II samples (30 μM), to which 2−30 equiv of either Co(II) or Fe(II) was added, were dialyzed extensively for 3 h at 4 °C against metal-free Hepes buffer. Upon ICP-AES analysis, 1.0 ± 0.1 equiv of cobalt or iron was tightly bound to the enzyme. These data suggest that only one Co(II) or one Fe(II) ion is tightly bound to *Pf*MetAP-II while the second metal ion is labile on the time scale of the buffer exchange (3 h, 4 °C). In a separate experiment, 2 equiv of Co(II) or Fe(II) were added to apo-*Pf*MetAP-II (30 μM), after which they were oxidized in air. The addition of hydrogen peroxide to the Co(II)-loaded *Pf*MetAP-II enzyme resulted in a distinct color change from violet/pink to brown, indicative of the formation of low-spin octahedral Co(III). Moreover, no EPR spectrum could be detected, consistent with diamagnetic Co(III) ions. After extensive dialysis at 4 °C with metal-free Hepes buffer, 2 equiv of cobalt or iron were found associated with *Pf*MetAP-II on the basis of ICP-AES analysis. These data suggest that Co(II) and Fe(II) are oxidized to Co(III) and Fe(III) forming [Co(III)Co(III)MetAP] and [Fe(III)Fe(III)(MetAP)] enzymes, both of which are inactive.

Substrate and Metal Ion Dependence on the Specific Activity of PfMetAP-II.

Kinetic constants and specific activities for both Co(II)- and Fe(II)-loaded *Pf*MetAP-II were determined for the peptide substrates MAS, MGMM, MSSHRWDW, and MP-*p*-NA (Table 1). Activity assays were performed in triplicate for 8−15 concentrations for each substrate (MAS, 0−60 mM; MGMM, 0−12 mM; MSSHRWDW, 0−12

mM; MP-*p*-NA, 0−1.2 mM). The product was quantified by HPLC or by monitoring the absorption at 405 nm for *p*-NA. The K_m and V_{max} values were obtained by nonlinear fitting of the data to the Michaelis−Menten equation. The k_{cat} and specific activity values were calculated using a molecular weight of 32850 and a molar absorptivity at 280 nm of 21650 M^{-1} cm^{-1}. The specific activities of *Pf*MetAP-II at 30 °C varied markedly on the basis of the substrate used. For the weakly binding tripeptide substrate MAS (K_m = 11.8 mM) the specific activity for Co(II)-loaded *Pf*MetAP-II was 35 units/mg whereas the tetrapeptide MGMM (K_m = 5.1 mM) exhibited a specific activity of 340 units/mg. These activities compare well with the only activity data reported to date for *Pf*MetAP-II of 30 units/mg toward the pentapeptide MPAAG. Fe(II) also activates *Pf*MetAP-II under anaerobic conditions. The trends in K_m and specific activity for Fe(II)-loaded *Pf*MetAP-II are similar to the Co(II)-loaded enzyme as well as the Fe(II)- and Co(II)-loaded *Ec*MetAP-I.

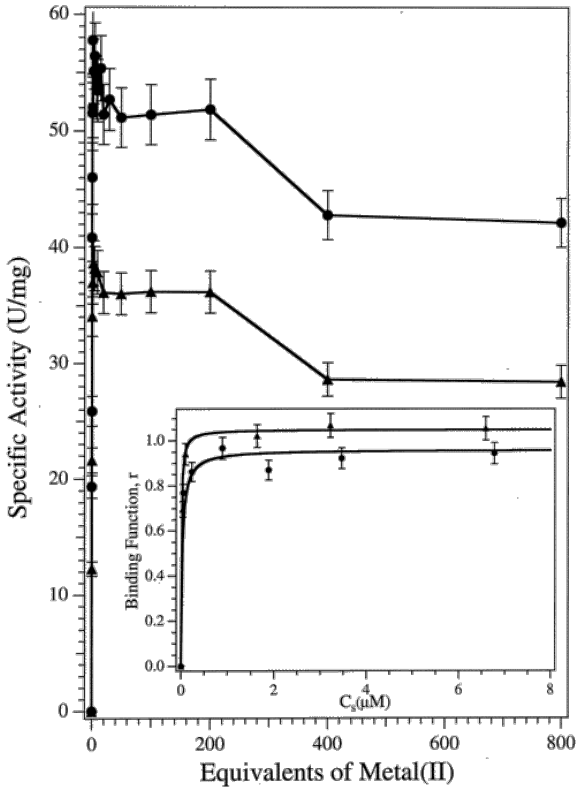

Figure 2 Plot of specific activity vs equivalents of added metal ion [(·) Co(II) and (▲) Fe(II)] to an 8.3 μM sample of *Pf*MetAP-II (25 mM Hepes buffer, pH 7.5, 150 mM KCl). Inset: Fits of the (·) Co(II) and (▲) Fe(II) activity data to eq 1.

Table 1: Kinetic Constants for Fe(II)- and Co(II)-Loaded *Pf*MetAP-II for Various Substrates at 30 °C and pH 7.5

metal	kinetic constants	MAS	MGMM	MSSHRWDW	MP-*p*-NA
Co(II)	K_m (mM)	11.8 ± 0.2	5.1 ± 0.3	2.0 ± 0.2	0.197 ± 0.015
	k_{cat} (s^{-1})	19	188	16	157
	k_{cat}/K_m (M^{-1} s^{-1})	1610	36900	8000	799500
	SA (units/mg)	35 ± 4	340 ± 8	29 ± 3	287 ± 6
Fe(II)	K_m (mM)	9.2 ± 0.4	5.0 ± 0.6	1.3 ± 0.2	0.135 ± 0.02
	k_{cat} (s^{-1})	14	153	22	46
	k_{cat}/K_m (M^{-1} s^{-1})	1520	30600	17200	340930
	V_{max} (nmol min^{-1})	16.8 ± 0.2	92 ± 9	6.7 ± 0.3	138 ± 4
	SA (units/mg)	25 ± 2	280 ± 10	41 ± 2	84 ± 2

Activity as a Function of Divalent Metal Ion Concentration.

The extent of hydrolytic activity exhibited by *Pf*MetAP-II was determined as a function of divalent metal ion concentration. Apo-*Pf*MetAP-II (8.3 μM) was incubated with varying amounts of Co(II) or Fe(II), and the level of catalytic activity was determined (Figure 2). Upon the addition of Co(II) to *Pf*MetAP-II under anaerobic conditions, the specific activity increased as a function of metal ion concentration up to 1 equiv of Co(II). Further additions of up to 5 equiv of Co(II) had no effect on the enzymatic activity. Interestingly, upon the addition of Co(II) to >83 μM (∼10 equivalents) the activity steadily decreased until ∼3.3 mM Co(II) had been added (400 equiv), at which time the activity was ∼30% of the maximum activity (Figure 2). Further additions of up to 800 equiv of Co(II) had no effect on the enzymatic activity. The decrease in activity could be due to the occupation of a second metal binding site or may be the result of chelation of the tetrapeptide substrate by excess divalent metal ions. Analogous behavior was also observed for Fe(II) (Figure 2).

The activity titration data for Co(II) and Fe(II) binding to *Pf*MetAP-II were fit to the equation (*24*):

$$r = pC_s/(K_d + C_s) \quad (1)$$

where *p* is the number of sites for which interaction with M(II) is governed by the intrinsic dissociation constant K_d and *r* is the binding function calculated by conversion of the fractional saturation (f_a) using the equation:

$$r = f_a p \quad (2)$$

C_S, the free metal concentration, was calculated using the equation:

$$C_s = C_{TS} - rC_A \quad (3)$$

where C_{TS} and C_A are the total and free molar concentrationsof metal and enzyme, respectively. A value for the dissociation constant (K_d) was obtained by fitting the data via an iterative process that allowed both K_d and *p* to vary (Figure 2, inset). The best fit obtained provided a *p* value of 1 and K_d values of 50 ± 15 and 20 ± 15 nM for Co(II)- and Fe(II)-substituted *Pf*MetAP-II, respectively.

Electronic Absorption Spectra of Co(II)-Bound PfMetAP-II.

The electronic absorption spectrum of a 1 mM sample of *Pf*MetAP-II with various amounts of Co(II) added was recorded under strict anaerobic conditions in 25 mM Hepes buffer, pH 7.5, and 150 mM KCl (Figure 3). The addition of one Co(II) ion to *Pf*MetAP-II provided an electronic absorption spectrum with λ_{max} values of 562 (ε_{562} = 110 M^{-1} cm^{-1}), 525 (ε_{525} = 72 M^{-1} cm^{-1}), and 590 nm (ε_{590} = 93 M^{-1} cm^{-1}). Further addition of Co(II) resulted in increases in absorption at 525 and 562 nm, consistent with the occupation of an additional metal binding site (Figure 3). The dissociation constant (K_d) for the second divalent metal binding site was obtained by fitting these data to eq 1 (Figure 4). The best fit obtained provided a *p* value of 1 and a K_d value of 0.35 ± 0.05 mM.

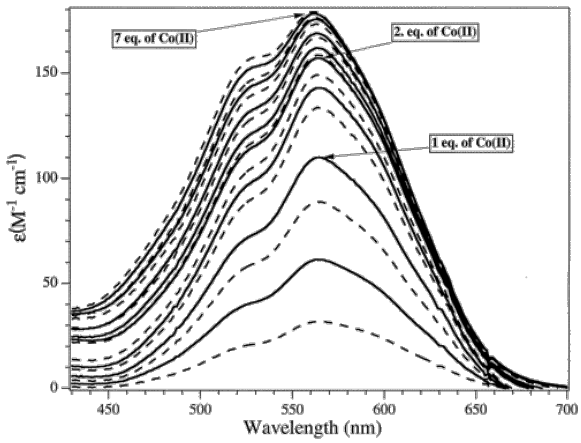

Figure 3 Electronic absorption spectral titration of 1 mM *Pf*MetAP-II (25 mM Hepes buffer, pH 7.5, 150 mM KCl) with Co(II) in 0.25 equiv increments.

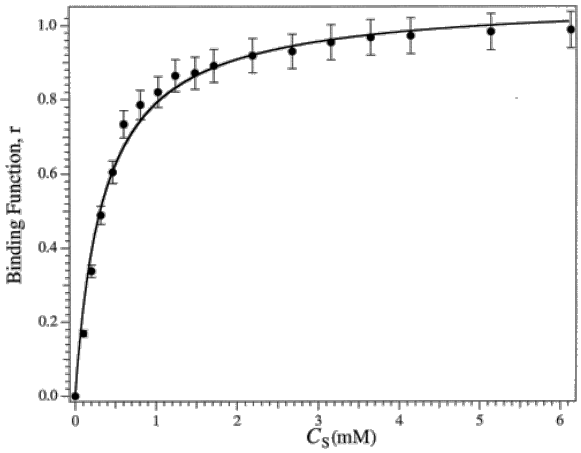

Figure 4 Plot of binding function, *r*, vs C_S (the concentration of free metal ions in solution) for λ_{562} of a 1 mM *Pf*MetAP-II sample (25 mM Hepes buffer, pH 7.5, and 150 mM KCl).

Temperature Dependence of the Hydrolysis of Met-Gly-Met-Met by PfMetAP-II. It was previously reported that *Pf*MetAP-II is stable at 75 °C for 60 min within the pH range 4.5−10.5. We have confirmed the thermal stability of *Pf*MetAP-II and have found that the optimal activity with MGMM as the substrate occurred at 85 °C in 25 mM Hepes, pH 7.5, and 150 mM KCl buffer. This provides us the unique opportunity to probe the thermodynamic properties of the *Pf*MetAP-II catalyzed hydrolysis of N-terminal methionine residues. The hydrolysis of MGMM was measured in triplicate between 25 and 85 °C at eight substrate concentrations ranging from 2 to 20 mM. From these data, K_m values were derived by fitting the experimental data to the Michaelis−Menten equation at each temperature studied (Figure 5B). The calculated specific activity values were plotted as a function of temperature between 25 and 85 °C (Figure 5A). The K_m and specific activity values for MGMM hydrolysis catalyzed by Co(II)- and Fe(II)-loaded *Pf*MetAP-II were found to increase with increasing temperature. *Pf*MetAP-II was stable at 85 °C for approximately 30 min before any loss in the enzymatic activity was detected. However, any loss in activity was fully reversible as a function of V_{max} for temperatures up to 70 °C. These data are very unusual since most enzymes undergo some denaturation at temperatures above 50 °C, resulting in a decrease in V_{max} (*22*).

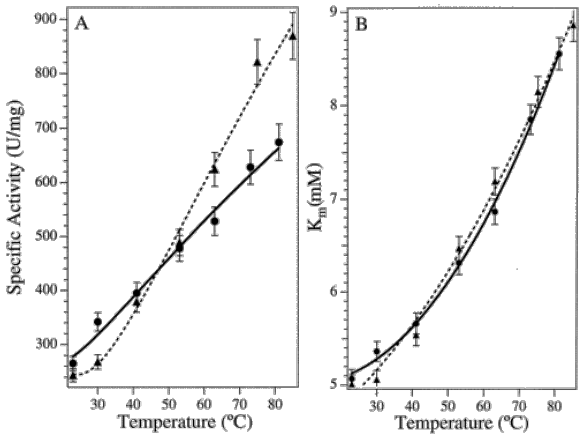

Figure 5 (A) Plot of specific activity (units/mg) of Co(II)- (·) and Fe(II)-loaded (▲) *Pf*MetAP-II vs temperature between 23 and 85 °C. Each data point is the sum of three activity measurements at pH 7.5, 25 mM Hepes buffer and 150 mM KCl, at substrate concentrations ranging from 2 to 20 mM. (B) K_m vs temperature (°C).

In a simple rapid equilibrium $V_{max}/[E] = k_p$, the first-order rate constant. Since the enzyme concentration was not altered over the course of the experiment, an Arrhenius plot can be constructed by plotting ln k_{cat} vs $1/T$ (Figure 6). A linear plot was obtained, indicating that the rate-limiting step does not change as the temperature is increased (*22*). From the slope of the line the activation energy, E_a, for temperatures between 296 and 358 K was calculated to be 13.3 kJ/mol for Co(II)-loaded *Pf*MetAP-II and 19.4 kJ/mol for Fe(II)-loaded enzyme. Since the slope of an Arrhenius plot is equal to $-E_{a1}/R$, where $R = 8.3145\ J \cdot K^{-1} \cdot mol^{-1}$, other thermodynamic parameters were calculated by the following relations: $\Delta G^{\ddagger} = -RT \ln(k_{cat}h/k_BT)$, $\Delta H^{\ddagger} = E_a - RT$, and $\Delta S^{\ddagger} = (\Delta H^{\ddagger} - \Delta G^{\ddagger})/T$, where k_B, h, and R are the Boltzmann, Planck, and gas constants, respectively (Table 2).

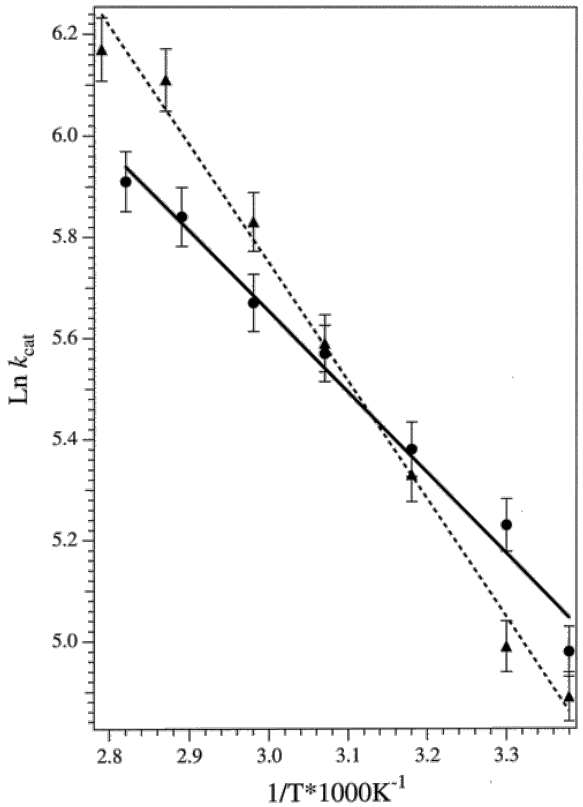

Figure 6 Arrhenius plot of ln k_{cat} vs $1/T$ for Co(II)- (·) and Fe(II)-loaded (▲) *Pf*MetAP-II. The solid and dashed lines are direct fits to the Arrhenius equation.

Table 2: Thermodynamic Parameters for the Hydrolysis of MGMM

enzyme	E_a (kJ/mol)	$\Delta H^{\ddagger}$ (kJ/mol)	$\Delta G^{\ddagger}$ (kJ/mol)	$\Delta S^{\ddagger}$ (J·mol^{-1}·K^{-1})
Co(II)-*Pf*MetAP	13.3	11	46	−119.7
Fe(II)-*Pf*MetAP	19.4	17	46	−99.7

Discussion

To effectively design small molecules that specifically target either type I or type II MetAP's and act as anticancer, antibacterial and/or antifungal agents, a knowledge of the variety and number of in vivo metal ions is required. Until recently, all MetAP's studied had been reported to require two Co(II) ions in a dinuclear active site (*13*−*16*). The conclusion that MetAP's are Co(II)-dependent enzymes was primarily arrived at from the reproducible observations that MetAP's show high activity in the presence of Co(II) when compared to the activity levels of other divalent metal ions (*23*). However, in all in vitro studies to date, Co(II) concentrations have been artificially increased to the millimolar range during purification. Moreover, several metalloproteases with active site ligands similar to those of MetAP's can substitute their native divalent metal ions with Co(II) in vitro, and in most cases, active and even hyperactive enzymes are obtained (*24, 25*). Because Co(II) is not abundant in nature and no biological systems require Co(II), except vitamin B_{12} where the cobalt ion resides in a very rigid corrin ring system (*24*), the suggestion that MetAP's are Co(II)-dependent hydrolases has been called into question (*17*, *18*, *26*). Walker and Bradshaw reported that the type I MetAP from *S. cerevisiae* is fully active with Zn(II) in the presence of millimolar concentrations of EDTA but that excess Zn(II) was inhibitory (*26*). More recently, *Ec*MetAP-I was shown to be completely inactive in the presence of Zn(II) ions but is fully active with only 1 equiv of Co(II) or Fe(II) (*18*). Unlike Co(II), Fe(II) is very abundant in nature and has many biological roles (*24*). On the basis of these data it was suggested that Fe(II) is the physiologically relevant metal ion for MetAP's (*18*). However, a recent study on *Hs*MetAP-II suggested that Co(II) is strictly required to activate this enzyme. Yang et al. (*20*) further suggested that type II MetAP's have different metal binding properties than type I MetAP's. Given the fact that the active site ligands in all MetAP's are strictly conserved (*27*) and the three X-ray crystal structures of both type I and type II MetAP's indicate that the active sites are superimposable (*13*−*16*), one would expect the metal binding properties of all MetAP's to be identical. Therefore, we have examined the metal binding properties of *Pf*MetAP-II so that a direct comparison of both type I and type II MetAP enzymes can be made under identical experimental conditions.

To effectively study the *Pf*MetAP-II enzyme by spectroscopic techniques, the gene that encodes *Pf*MetAP-II was cloned and placed into a pET 27b(+) expression vector. After overexpression and purification, a 5-fold increase in enzyme production was observed, allowing 100 mg of purified *Pf*MetAP-II to be obtained from 5 L fermentation growth. This increase in *Pf*MetAP-II overproduction provides us the opportunity to perform a detailed structure−function analysis of type II MetAP's via detailed kinetic, spectroscopic, and X-ray crystallographic studies. The as-purified *Pf*MetAP-II, to which no exogenous metal ions or EDTA was added, was shown to have ∼1.2 equiv of zinc and ∼0.1 equiv of iron present by ICP-AES analysis. This enzyme had a specific activity of ∼5 units/mg, a 60-fold decrease from the fully loaded Co(II) or Fe(II) enzymes. When two additional equivalents of Zn(II) were added to the as-purified *Pf*MetAP-II, no activity could be detected. Similar results were reported for *Hs*MetAP-II in which 0.78 ppm of Zn(II) ([*Hs*MetAP-II]:[Zn(II)] = 1:1) was found after purification but the enzyme was essentially inactive (*20*). Moreover, *Ec*MetAP-I is completely inactive in the presence of Zn(II). Interestingly, the as-purified *Pf*MetAP-II contained ∼10% of the required amount of iron for activity (*17*). No cobalt could be detected within the 0.03 ppm detection limit for ICP-AES. Given the air sensitivity of the Fe(II) center in MetAP's, it is logical that the as-purified *Pf*MetAP-II enzyme exhibited only ∼2% of the activity

observed for Fe(II)-loaded *Pf*MetAP-II under strict anaerobic conditions. These data are the first to directly indicate that MetAP's are Fe(II)-dependent enzymes. The low level of iron detected in the as-purified *Pf*MetAP-II enzyme is likely the result of overwhelming the iron transport system during overexpression. The combination of these data with previously reported whole cell studies on *Ec*MetAP-I (*18*) strongly suggests that the in vivo metal ion for all MetAP's is not Zn(II) or Co(II) but is, in fact, Fe(II).

*Pf*MetAP-II can be fully activated by both Co(II) or Fe(II) (Table 1). The kinetic parameters display similarities to *Ec*MetAP-I and *Hs*MetAP-II (*17, 20*). Moreover, the observed K_m values for Fe(II)-loaded *Pf*MetAP-II are almost always smaller than those for the Co(II)-loaded enzyme. The substrate binding affinity (K_m) is largely affected by the amino acid in the P1‘ position as well as the length of the polypeptide used as the substrate. For the substrates MAS, MGMM, and MSSHRWDW, the K_m values are in the millimolar range, but the K_m value decreased for both Co(II)- and Fe(II)-loaded *Pf*MetAP-II as the peptide chain length increased. For comparison, assayed in the presence of 0.5 mM Co(II), *Sc*MetAP-I showed a K_m value of 6.6 mM for the tetrapeptide MGMM while the K_m value toward the octapeptide MSSHNTDT was found to be 0.019 mM (*31*). This difference in K_m is likely because a longer peptide can interact with other amino acid residues in or near the active site.

X-ray crystallographic studies on *Hs*MetAP-II, *Pf*MetAP-II, and *Ec*MetAP-I have all shown that two Co(II) ions reside in a dinuclear active site with a M−M distance ranging from 2.9 to 3.1 Å (*13*−*16*). However, it has also been shown that one metal ion is loosely associated with *Ec*MetAP-I, *Sc*MetAP-I, and the human homologue of the rat initiation factor 2 associated protein (*17*, *26*, *28*). Recent EXAFS studies on *Ec*MetAP-I revealed the lack of a dinuclear site at enzyme concentrations of 1 mM even in the presence of excess divalent metal ions (*19*). These data strongly suggest that, under physiological conditions, a dinuclear active site does not form in MetAP's. The observation that MetAP's are dinuclear metalloproteases is based solely on X-ray crystallographic studies in which at least a 10-fold excess of Co(II) was added to millimolar concentrations of enzyme during crystallization (*13*−*16*). The lack of a dinuclear center is also consistent with ICP-AES analyses of *Ec*MetAP-I, which indicated that, upon the addition of divalent metal ions, only one is tightly bound per enzyme molecule (*17*). ICP-AES analyses of *Pf*MetAP-II also revealed only one divalent metal ion tightly bound per enzyme molecule, under anaerobic conditions, similar to *Ec*MetAP-I.

Titration of apo-*Pf*MetAP-II (8.3 μM) with either Co(II) or Fe(II) under anaerobic conditions revealed that both metal ions fully activate the enzyme after the addition of only 1 equiv (Figure 2; inset). Further additions of up to 5 equiv of Co(II) or Fe(II) did not alter the enzymatic activity. Fits of these titration data provided dissociation constants (K_d) for the first metal binding site of 50 and 20 nM for Co(II)- and Fe(II)-loaded *Pf*MetAP-II, respectively. Since only one metal ion is bound to the enzyme active site, these K_d values correspond to the microscopic binding constants for the binding of a single metal ion to *Pf*MetAP-II. K_d values of 300 and 200 nM have been reported for Co(II)- and Fe(II)-loaded *Ec*MetAP-I (*17*), respectively, which are similar in magnitude to those observed for *Pf*MetAP-II. These K_d values are also similar to K_d values obtained for several other hydrolytic enzymes that contain carboxylate-rich active sites. For example, the K_d value for the first metal binding site of the aminopeptidase from *A. proteolytica* is 1 nM (*29*), the clostridial aminopeptidase exhibits a K_d value of 2 μM (*30*), the clostridial AMPP has a reported K_d value of 7 μM (*30*), and the β-lactamase from *Bacillus cereus* has a divalent metal ion K_d value of 620 nM (*31*).

The addition of 8 equiv of divalent metal ions to *Pf*MetAP-II up to 400 equiv, inhibited the enzymatic activity by ∼30%. Similar results were observed for *Ec*MetAP-I, *Sc*MetAP-I, and *Hs*MetAP-II in which the addition of excess divalent metal ions inhibited the enzymatic activity (*17*, *20*, *26*). These data suggest that the binding of a second metal ion to all MetAP's is inhibitory, which would imply that the second metal ion either has no catalytic role or is regulatory. Inhibition of catalytic activity by excess divalent metal ions has also been observed for other mononuclear metalloenzymes such as carboxypeptidase *Taq* when overexpressed in *E. coli* (*32*), bovine carboxypeptidase A (*33, 34*), and thermolysin (*35*). Inhibition of carboxypeptidase A was attributed to excess

metal ion binding to an amino acid residue near the metallo active site that was involved in catalysis (*33*). In addition, the authors proposed that a bridging hydroxide, inserted between the two metal ions, forming a dinuclear site, was the result of the second metal ion binding event. This proposal was corroborated by X-ray crystallography where the structures of carboxypeptidase A as well as thermolysin in the presence of excess metal ion revealed two coordinated metal ions forming a (μ-hydroxo)dizinc(II) core with a Zn−Zn distance of 3.48 and 3.2 Å, respectively (*35*−*37*). Therefore, the observation that the addition of excess metal ions to *Ec*MetAP-I, *Sc*MetAP-I, *Hs*MetAP-II, and *Pf*MetAP-II inhibited enzymatic activity suggests that inhibition is likely due to the occupation of the second metal binding site, similar to carboxypeptidase A.

To further examine the metal binding properties of *Pf*MetAP-II, the electronic absorption spectra of Co(II)-loaded *Pf*MetAP-II (1 mM) were recorded. Upon the addition of 1 equiv of Co(II) under anaerobic conditions, three resolvable d−d transitions at 525, 562, and 590 nm (ε = 72, 110, and 93 M^{-1} cm^{-1}, respectively) were observed. On the basis of ligand-field theory (*25*), these data indicate that the first Co(II) ion to bind to *Pf*MetAP-II resides in a pentacoordinate site, in agreement with X-ray crystallography (*14*). These data are also nearly identical to those previously reported for *Ec*MetAP-I (*17*), further suggesting the similarity in the active sites of both type I and type II MetAP's. Upon the addition of 2 equiv of Co(II) the absorption spectrum does not change appreciably but the molar absorptivity continues to increase until more than 7 equiv of Co(II) have been added. These data suggest that the second Co(II) ion also resides in a pentacoordinate environment but that it is loosely bound to the enzyme. Fits of the two absorption maxima at 525 and 562 nm provided a K_d at pH 7.5 for the second metal binding site of 0.35 mM. Therefore, the ability of *Pf*MetAP-II to bind one vs two divalent metal ions is very different (17.5×10^3 times), indicating that under physiological conditions the second metal binding site is unoccupied. On the basis of these data, we propose that *Pf*MetAP-II functions as a mononuclear hydrolase in vivo similar to that of *Ec*MetAP-I (*17*). However, Yang et al. (*20*) recently suggested that *Hs*MetAP-II requires two Co(II) ions for full enzymatic activity to be achieved, based on the titration of Co(II) ions under aerobic conditions into a 100 nM *Hs*MetAP-II sample with 1 equiv of tightly bound Zn(II). On the basis of simple equilibrium principles, as outlined in Scheme 1, and the assumption that the K_d value for the first metal binding site in *Hs*MetAP-II is 50 nM, the value reported herein for *Pf*MetAP-II, under the experimental conditions reported by Yang et al. (*20*), *Hs*MetAP-II, would only have ∼0.5 equiv of Co(II) bound at a Co(II) concentration of 100 nM. This calculation assumes that *Hs*MetAP-II is apo but, in fact, 1 equiv of Zn(II) was present which likely competes with Co(II) binding at the active site. Therefore, the low level of activity observed for *Hs*MetAP-II in the presence of 1 equiv of Co(II) (100 nM) is quite reasonable as is the observed increase in activity in the presence of 100 equiv of Co(II) (10 μM). At a Co(II) concentration of 10 μM, the total Co(II) concentration would now be at least 10-fold greater than the equilibrium constant, providing an *Hs*MetAP-II enzyme that has one Co(II) binding site >95% filled. Therefore, the data reported by Yang et al. (*20*) are completely consistent with *Hs*MetAP-II functioning in vivo as a mononuclear metalloprotease, identical to *Ec*MetAP-I and *Pf*MetAP-II.

$$\mathrm{Co(II)} + Pf\mathrm{MetAp-II} \underset{k_{-1}}{\overset{k_1}{\rightleftharpoons}} [\mathrm{Co(II)\_}(Pf\mathrm{MetAP-II})]$$

$$\mathrm{Co(II)} + [\mathrm{Co(II)\_}(Pf\mathrm{MetAP-II})] \underset{k_{-2}}{\overset{k_2}{\rightleftharpoons}} [\mathrm{Co(II)Co(II)}(Pf\mathrm{MetAP-II})]$$

Scheme 1

An important question in understanding the cleavage of N-terminal methionine residues from polypeptide chains by MetAP's is “what is the rate-limiting step in the catalytic reaction?” Since *Pf*MetAP-II is stable at 75 °C for 1 h, *Pf*MetAP-II provides the unique opportunity to determine the activation parameters of the $ES^{\ddagger}$ complex over a wide temperature range. Construction of an Arrhenius plot from the temperature dependence

of *Pf*MetAP-II activity indicates that the rate-limiting step does not change as a function of temperature and is product release (*22*). The activation energy (E_a) for the activated ES‡ complex is 13.3 and 19.4 kJ/mol for Co(II)- and Fe(II)-loaded *Pf*MetAP-II, respectively. These data are approximately one-half the E_a reported for the aminopeptidase from *A. proteolytica* (36.5 kJ/mol) which has an activation energy similar to those of Pronase and both thermolysin and carboxypeptidase A (*38*−*40*). The enthalpy of activation calculated over the temperature range 25−85 °C is 11.0 and 17.0 kJ/mol for Co(II)- and Fe(II)-loaded *Pf*MetAP-II, respectively, while the entropy of activation was found to be −119.7 and −99.7 J mol^{-1}·K^{-1} for Co(II)- and Fe(II)-loaded *Pf*MetAP-II, respectively, at 25 °C. The positive enthalpy is indicative of a conformation change upon substrate binding, likely due to the energy of bond formation and breaking during nucleophilic attack on the scissile carbonyl carbon of the substrate. On the other hand, the large negative entropy value suggests that some of the molecular motions are lost upon ES‡ complex formation possibly due to hydrogen bond formation between catalytically important amino acids and the substrate. All of these factors contribute to the large positive free energy of activation. Interestingly, Fe(II)-loaded *Pf*MetAP-II is 1.4 times more active than Co(II)-loaded *Pf*MetAP-II at 85 °C. However, the K_m values for both Co(II)- and Fe(II)-loaded *Pf*MetAP-II are identical, within experimental error, indicating that Fe(II)-loaded *Pf*MetAP-II is a much better catalyst at the optimum growth temperature of *P. furiosus* (85 °C). These data further suggest that Fe(II) is the physiologically relevant metal ion.

In conclusion, the data presented herein provide new evidence that MetAP's are Fe(II) metalloproteases (Figure 7) on the basis of the fact that the as-purified *Pf*MetAP-II contains both iron and zinc; however, Zn(II) does not activate the enzyme, but Fe(II) provides a fully active enzyme, under anaerobic conditions. *Pf*MetAP-II, like *Ec*MetAP-I, is fully active in the presence of 1 equiv of Co(II) or Fe(II), and excess divalent metal ions inhibit enzymatic activity. Furthermore, electronic absorption spectra of [Co$_2$(*Pf*MetAP-II)] like [Co$_2$(*Ec*MetAP-I)] suggest that the first Co(II) binding site is five coordinate, consistent with X-ray crystallographic data. The only difference observed in divalent metal binding properties between type I and type II MetAP's is the magnitude of the K_d values for both metal binding sites. The K_d values observed for type II MetAP's are approximately 10 times smaller than those observed for type I enzymes. These data suggest that the 62 amino acid insert found in type II MetAP's alters the enzyme structure in such a way as to increase the enzyme's affinity for divalent metal ions. Combination of the data presented herein with divalent metal binding data previously reported for all MetAP's, including *Hs*MetAP-II, suggests that type II MetAP's bind metal ions in exactly the same way as type I MetAP's. These data are not surprising since all MetAP active site ligands are strictly conserved and the active sites of the three crystallographically characterized MetAP's are completely superimposable. Therefore, all MetAP's likely function as mononuclear Fe(II) metalloproteases under physiological conditions.

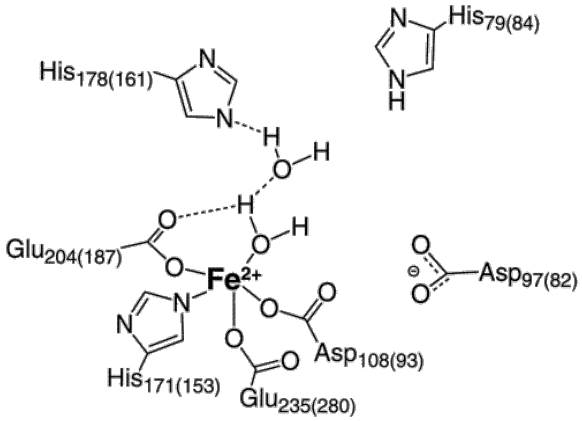

Figure 7 Proposed active site structure of Fe(II)-loaded MetAP's. The amino acid numbering is for *Ec*MetAP-I with the amino acid numbers for *Pf*MetAP-II in parentheses.

References

1 Bradshaw, R. A. (1989) *Trends Biochem. Sci.14*, 276−279.

2 Meinnel, T., Mechulam, Y., and Blanquet, S. (1993) *Biochimie75*, 1061−1075.

3 Bradshaw, R. A., Brickey, W. W., and Walker, K. W. (1998) *Trends Biochem. Sci.23*, 263−267.

4 Arfin, S. M., and Bradshaw, R. A. (1988) *Biochemistry27*, 7979−7984.

5 Hirel, P.-H., Schmitter, J.-M., Dessen, P., Fayat, G., and Blanquet, S. (1989) *Proc. Natl. Acad. Sci. U.S.A.86*, 8247−8251.

6 Chang, S.-Y. P., McGary, E. C., and Chang, S. (1989) *J. Bacteriol.171*, 4071−4072.

7 Miller, C. G., Kukral, A. M., Miller, J. L., and Movva, N. R. (1989) *J. Bacteriol.171*, 5215−5217.

8 Li, X., and Chang, Y.-H. (1995) *Proc. Natl. Acad. Sci. U.S.A.92*, 12357−12361.

9 Taunton, J. (1997) *Chem. Biol.4*, 493−496.

10 Griffith, E. C., Su, Z., Turk, B. E., Chen, S., Chang, Y.-H., Wu, Z., Biemann, K., and Liu, J. O. (1997) *Chem. Biol.4*, 461−471.

11 Sin, N., Meng, L., Wang, M. Q., Wen, J. J., Bornmann, W. G., and Crews, C. M. (1997) *Proc. Natl. Acad. Sci. U.S.A.94*, 6099−6103.

12 Lowther, W. T., McMillen, D. A., Orville, A. M., and Matthews, B. W. (1998) *Proc. Natl. Acad. Sci. U.S.A.95*, 12153−12157.

13 Liu, S., Widom, J., Kemp, C. W., Crews, C. M., and Clardy, J. (1998) *Science282*, 1324−1327.

14 Tahirov, T. H., Oki, H., Tsukihara, T., Ogasahara, K., Yutani, K., Ogata, K., Izu, Y., Tsunasawa, S., and Kato, I. (1998) *J. Mol. Biol.284*, 101−124.

15 Lowther, W. T., Orville, A. M., Madden, D. T., Lim, S., Rich, D. H., and Matthews, B. W. (1999) *Biochemistry38*, 7678−7688.

16 Roderick, S. L., and Matthews, B. W. (1993) *Biochemistry32*, 3907−3912.

17 D'souza, V. M., Bennett, B., Copik, A. J., and Holz, R. C. (2000) *Biochemistry39*, 3817−3826.

18 D'souza, V. M., and Holz, R. C. (1999) *Biochemistry38*, 11079−11085.

19 Cosper, N. J., D'souza, V., Scott, R., and Holz, R. C. (2001) *Biochemistry40*, 13302.

20 Yang, G., Kirkpatrick, R. B., Ho, T., Zhang, G.-F., Liang, P.-H., Johanson, K. O., Casper, D. J., Doyle, M. L., Marino, J. P., Thompson, S. K., Chen, W., Tew, D. G., and Meek, T. D. (2001) *Biochemistry40*, 10645−10654.

21 Tsunasawa, S., Izuy, Y., Miyagi, M., and Kato, I. (1997) *J. Biochem.122*, 843−850.

22 Segel, I. H. (1975) *Enzyme Kinetics: Behavior and analysis of rapid equilibrium and steady-state enzyme systems*, 1st ed., John Wiley & Sons, New York.

23 Ben-Bassat, A., Bauer, K., Chang, S.-Y., Myambo, K., Boosman, A., and Chang, S. (1987) *J. Bacteriol.169*, 751−757.

24 Holm, R. H., Kennepohl, P., and Solomon, E. I. (1996) *Chem. Rev.96*, 2239−2314.

25 Bertini, I., and Luchinat, C. (1984) *Adv. Inorg. Biochem.6*, 71−111.

26 Walker, K. W., and Bradshaw, R. A. (1998) *Protein Sci.7*, 2684−2687.

27 Lowther, W. T., and Matthews, B. W. (1999) *Proteins: Struct., Funct*., *Genet*. (submitted for publication).

28 Li, X., and Chang, Y.-H. (1996) *Biochem. Biophys. Res. Commun.227*, 152−159.

29 Prescott, J. M., and Wilkes, S. H. (1976) *Methods Enzymol.45B*, 530−543.

30 Fleminger, G., and Yaron, A. (1984) *Biochim. Biophys. Acta789*, 245−256.

31 de Seny, D., Heinz, U., Wommer, S., Kiefer, M., Meyer-Klaucke, W., Galleni, M., Frère, J.-M., Bauer, R., and Adolph, H.-W. (2001) *J. Biol. Chem.276*, 45065−45078.

32 Lee, S. H., Taguchi, H., Yoshimura, E., Minagawa, E., Kaminogawa, S., Ohta, T., and Matsuzawa, H. (1994) *Biosci. Biotechnol. Biochem.58*, 1490−1495.

33 Larsen, K. S., and Auld, D. S. (1989) *Biochemistry28*, 9620−9625.

34 Larsen, K. S., and Auld, D. S. (1991) *Biochemistry30*, 2613−2618.
35 Holland, D. R., Hausrath, A. C., Juers, D., and Matthews, B. W. (1995) *Protein Sci.4*, 1955−1965.
36 Gomez-Ortiz, M., Gomis-Ruth, F. X., Huber, R., and Aviles, F. X. (1997) *FEBS Lett.400*, 336−340.
37 Bukrinsky, J. T., Bjerrum, M. J., and Kadziola, A. (1998) *Biochemistry37*, 16555−16564.
38 Lumry, R., Smith, E. L., and Glantz, R. R. (1951) *J. Am. Chem. Soc.73*, 4330−4340.
39 Kunugi, S., Hirohara, H., and Ise, N. (1982) *Eur. J. Biochem.124*, 157−163.
40 Wu, C.-H., and Lin, W.-Y. (1995) *J. Inorg. Biochem.57*, 79−89.

1 Abbreviations: MetAP's, methionyl aminopeptidases; PMSF, phenylmethanesulfonyl fluoride; IPTG, isopropyl β-d-thiogalactoside; Hepes, 4-(2-hydroxyethyl)-1-piperazineethanesulfonic acid; Tris, tris(hydroxymethyl)aminomethane; SDS−PAGE, sodium dodecyl sulfate−polyacrylamide gel electrophoresis; HPLC, high-performance liquid chromatography; TFA, trifluoroacetic acid; ICP-AES, inductively coupled plasma atomic emission spectrometry; MAS, Met-Ala-Ser; MGMM, Met-Gly-Met-Met; MSSHRWDW, Met-Ser-Ser-His-Arg-Trp-Asp-Trp; MP-*p*-NA, methionylprolyl-*p*-nitroanilide.